Eur. Phys. J. C 10, 689–696 (1999)
Digital Object Identifier (DOI) 10.1007/s100529900160

THE EUROPEAN PHYSICAL JOURNAL C
© Springer-Verlag 1999

Total γ^*p cross section

E. Gotsman[a], E. Levin[b], U. Maor[c], E. Naftali[d]

School of Physics and Astronomy, Raymond and Beverly Sackler Faculty of Exact Science, Tel Aviv University, Tel Aviv, 69978, Israel

Received: 11 April 1999 / Published online: 28 September 1999

Abstract. This paper shows that the approach based on Gribov's ideas for photon–proton interaction is able to describe the experimental data over a wide range of photon virtualities $Q^2 = 0$–$100\,\mathrm{GeV}^2$ and energies $\sqrt{s} = W = 3$–$300\,\mathrm{GeV}$. A simple model is suggested which provides a quantitative way of describing the matching between short and long distances (between "soft" and "hard" processes) in photon–proton interaction at high energy. The main results of our analysis are: (i) the values of the separation parameters differentiating the soft and hard interactions are determined; (ii) the additive quark model can be used to calculate the soft contribution to the photon–proton interaction; (iii) a good description of the ratio $\sigma_{\mathrm{L}}/\sigma_{\mathrm{T}}$ is obtained; and (iv) a considerable contribution of the soft process at large Q^2, and of hard processes at small Q^2 was found.

1 Introduction

The rich and high precision data on deep inelastic ep scattering at HERA [1,2], covering both low and high Q^2 regions, lead to a theoretical problem of matching the non-perturbative ("soft") and perturbative ("hard") QCD domains. This challenging problem has been under close investigation over the past two decades, starting from the pioneering paper of Gribov [3] (see also [4]).

Based on Gribov's general approach, one can interpret two time sequences of the γ^*p interaction (see Fig. 1):

1. First, the γ^* fluctuates into a hadron system (quark–antiquark pair to the lowest order) well before the interaction with the target.
2. Then, the converted quark–antiquark pair (or hadron system) interacts with the target.

These two stages are expressed explicitly in the double dispersion relation suggested in [3]:

$$\sigma(\gamma^* N) = \frac{\alpha_{\mathrm{em}}}{3\pi}\int \frac{\Gamma(M^2)\mathrm{d}M^2}{(Q^2+M^2)}\sigma(M^2,M'^2,s)\frac{\Gamma(M'^2)\mathrm{d}M'^2}{(Q^2+M'^2)}, \quad (1)$$

where M and M' are the invariant masses of the incoming and outgoing quark–antiquark pairs, $\sigma(M^2,M'^2,s)$ is the cross section of a $\mathrm{q\bar{q}}$ interaction with the target, and the vertices $\Gamma^2(M^2)$ and $\Gamma^2(M'^2)$ are given by $\Gamma^2(M^2) = R(M^2)$, where $R(M^2)$ is the ratio:

$$R(M^2) = \frac{\sigma(\mathrm{e^+e^-}\to\text{hadrons})}{\sigma(\mathrm{e^+e^-}\to\mu^+\mu^-)}, \quad (2)$$

which has been measured experimentally. For large masses (M, $M' \gg M_0$) we have $\Gamma(M^2 \geq M_0^2) \times \Gamma(M'^2 \geq M_0^2) \longrightarrow R(M^2 \geq M_0^2) = 2$, where we assume that that the number of colors $N_{\mathrm{c}} = 3$. M_0 is a typical mass (a separation parameter), which is of the order of $M_0 = 1$ GeV, determined directly from the experimental data [5].

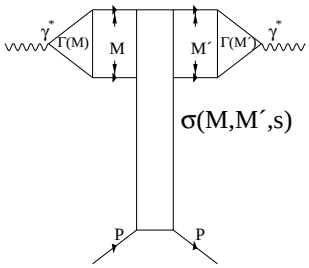

Fig. 1. The generalized Gribov's formula

The key problem in all approaches utilizing (1) is the description of the cross section $\sigma(M^2,M'^2,s)$. In this paper we follow the approach suggested in [6], which is based on the ideas of Badelek and Kwiecinski [7]. Below we list the main steps of this approach.

1. We introduce $M_0 \approx 1\,\mathrm{GeV}$ in the integrals over M and M' which plays the role of a separation parameter. For M, $M' > M_0$ the quark–antiquark pair are produced at short distances ($r_\perp \propto 1/M < \frac{1}{M_0}$), while for M, $M' < M_0$ the distance between the quark and

[a] e-mail: gotsman@post.tau.ac.il
[b] e-mail: leving@post.tau.ac.il
[c] e-mail: maor@post.tau.ac.il
[d] e-mail: erann@post.tau.ac.il

antiquark is too long ($r_\perp \propto \frac{1}{M} > \frac{1}{M_0}$), and we cannot treat this $q\bar{q}$ pair in perturbative QCD (pQCD). Actually, we cannot even describe the produced hadron state as a $q\bar{q}$ pair.

2. For M, $M' < M_0$ we use the additive quark model (AQM) [8] in which

$$\sigma(M^2, M'^2, s) = \sigma_{\rm N}^{\rm soft}(M^2, s)\delta(M^2 - M'^2) = (\sigma_{\rm tot}(qN) + \sigma_{\rm tot}(\bar{q}N))\,\delta(M^2 - M'^2) \quad (3)$$

The above assumption allows us to simplify the Gribov formula of (1):

$$\sigma(\gamma^* N) = \frac{\alpha_{\rm em}}{3\pi}\int \frac{R(M^2)M^2 {\rm d}M^2}{(Q^2+M^2)^2}\sigma_N(M^2, s)\,. \quad (4)$$

3. For M, $M' > M_0$ we consider the system with mass M and/or M' as a short-distance quark–antiquark pair, and describe its interaction with the target in pQCD (see Fig. 2).
The exact formulas for $\sigma^{\rm hard}(M^2, M'^2, s)$ are given below (see also [6]), but one can see from Fig. 2 that this interaction can be expressed through the gluon structure function, and it is *not* diagonal with respect to the masses, contrary to the soft interaction of a hadron system with small mass.
4. In principle, the short distance between the quark and antiquark leads to short distances in the gluon–nucleon interaction. However, the typical distance of the gluon interaction $r_G \propto 1/l_\perp$ (see Figs. 1 and 2) is larger than the size of the quark–antiquark pair and $l_\perp < k_\perp$. It turns out that the calculation with $M_0 \sim 1\,{\rm GeV}$ demands a new scale in the gluon–nucleon interaction. We introduce it assuming that the gluon structure function $xG(x, l_\perp^2)$ behaves as $xG(x, \mu^2) \times \frac{l_\perp^2}{\mu^2}$ for $l_\perp^2 \le \mu^2$. This means that we assume that the gluon–hadron total cross section is not equal to zero for long distances (in the soft kinematic region). It should be stressed that we introduce two scales for soft nonperturbative interactions, distinguishing between quark and gluon interactions. The two scales appear naturally in our models for soft, nonperturbative interactions. For example, in the AQM, which we use for $\sigma^{\rm soft}$, these two scales are the size of a hadron (distance between the quark and antiquark), and the size of the constituent quark, which is related to gluon interaction scale.
5. As has been discussed, we use the AQM [see (3)] to calculate $\sigma^{\rm soft}$. For the vector meson cross section the AQM leads to

$$\sigma_{\rm R} = \frac{1}{2}\left(\sigma(\pi^+ p) + \sigma(\pi^- p)\right). \quad (5)$$

For the pion–proton cross section, we use the Donnachie–Landshoff Reggeon parameterization [9], with an energy variable which is appropriate for the interaction of a hadronic system of mass M with the target (see [6] for details).

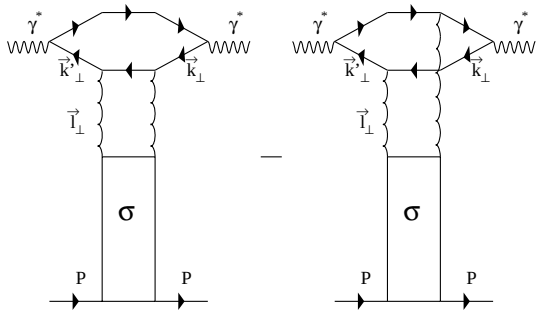

Fig. 2. "Hard" contribution to $\sigma(M^2, M'^2, s)$ in perturbative QCD

$$\sigma_{M^2 N}(s) = A\left(\frac{1}{x_M}\right)^{\alpha_{\mathbb{P}}(0)-1} + B\left(\frac{1}{x_M}\right)^{\alpha_{\mathbb{R}}(0)-1}, \quad (6)$$

with

$$\begin{aligned} \alpha_{\mathbb{P}} &= 1.079 \\ \alpha_{\mathbb{R}} &= 0.55 \\ x_M &= \frac{M^2}{s} \\ A &= 13.1\,{\rm mb} \\ B &= 41.08\,{\rm mb}\,. \end{aligned} \quad (7)$$

The values of A and B are chosen so that (6) is valid for the ρ–proton interaction. Using (6) in Gribov formula (4), we derive the soft transverse contribution to $\sigma(\gamma^* p)$:

$$\sigma_{\rm T}^{\rm soft} = \frac{\alpha_{\rm em}}{3\pi}\int_0^{M_0^2}\frac{R(M^2)M^2{\rm d}M^2}{(Q^2+M^2)^2} \times\left\{A\left(\frac{1}{x_M}\right)^{\alpha_{\mathbb{P}}(0)-1} + B\left(\frac{1}{x_M}\right)^{\alpha_{\mathbb{R}}(0)-1}\right\}. \quad (8)$$

It has been shown in [6] that even though the simple model discussed above reproduces the main features of the experimental data, it has several deficiencies:

- The calculations of the soft cross section appeared to overestimate the data, and to overcome this, the soft contribution was multiplied by a factor $\kappa = 0.6$. There is no physical justification for such a small value.
- The contribution of a longitudinal polarized virtual photon to $\sigma(\gamma^* p)$ was neglected.
- An old GRV '94 parameterization was used for the gluons' distribution inside the proton. This gave an energy dependence of $\sigma(\gamma^* p)$ that is steeper than the published data.

In the present paper, we reexamine these points developing a formalism which also takes into account $\sigma_{\rm L}$, the longitudinal part of $\sigma(\gamma^* p)$, for both the soft and the hard components. We find that the contribution of $\sigma_{\rm L}$ significantly improves the energy dependence of $\sigma(\gamma^* p)$, and is in good agreement with the data for $x < 10^{-2}$.

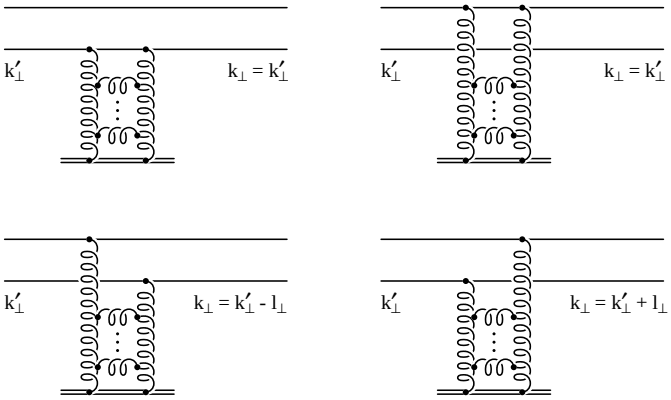

Fig. 3. Diagrams which contribute to the scattering of a $\bar{\mathrm{q}}$q pair off the target proton

A similar approach to photon–proton interaction was developed in [10] where quite different scales have been introduced. The goal of such an approach (see [6,7,10]) is to find parameters that separate the long-distance (nonperturbative) and short-distance (perturbative) interactions in QCD. A similar philosophy to ours is used in [11], where an attempt is made to describe photon–proton interactions, with the assumption that the main contribution stems from short distances; the long-distance interaction appears as a result of the shadowing corrections.

The description of $\sigma(\gamma^*\mathrm{p})$ can be achieved in quite a different way with the generalized vector dominance model [4] or a Regge-motivated fit of the experimental data [12, 13]. In these approaches, one loses the explicit connection with the microscopic theory, which makes further theoretical interpretation of the results rather difficult.

2 Description of the model

2.1 The contribution of a transverse polarized photon

As we have discussed previously, the main assumption of our model is that $\sigma(M^2, M'^2, s)$ in (1) can be calculated as

$$\sigma(M^2, M'^2, s) = \sigma_{\mathrm{N}}^{\mathrm{soft}}(M^2 < M_0^2, s)\,\delta(M^2 - M'^2) + \sigma^{\mathrm{hard}}(M^2 > M_0^2, M'^2 > M_0^2, s)\,. \quad (9)$$

In the previous section, we discussed the calculation of σ^{soft}. Now we present for completeness our formulas for σ^{hard}, which have been given in [6]. The pQCD contribution for σ_{T}, within the framework of the two gluon model, is illustrated in the four diagrams shown in Fig. 3. The production amplitude $\mathcal{M}_{\lambda\lambda'}$ of the $\bar{\mathrm{q}}$q can be factorized into the wave function $\psi_{\lambda\lambda'}$ of the $\bar{\mathrm{q}}$q system inside the virtual photon, and the amplitude $\mathcal{T}_{\lambda\lambda'}$ for the scattering of the $\bar{\mathrm{q}}$q pair off the proton:

$$\mathcal{M}_{\lambda\lambda'}(k_\perp, z) = \sqrt{N_{\mathrm{c}}}\int \mathrm{d}^2{k_\perp}' \int_0^1 \mathrm{d}z' \psi_{\lambda\lambda'}({k_\perp}', z') \times \mathcal{T}_{\lambda\lambda'}({k_\perp}', z'; k_\perp, z)\,. \quad (10)$$

The transition amplitude $\mathcal{T}_{\lambda\lambda'}$ for the four contributions is:

$$\mathcal{T}_{\lambda\lambda'}({k_\perp}', k_\perp) = \mathrm{i}\frac{4\pi s}{2N_{\mathrm{c}}}\int \frac{\mathrm{d}^2\ell_\perp}{\ell_\perp^4}\Big[2\delta(\boldsymbol{k}'_\perp - \boldsymbol{k}_\perp) - \delta(\boldsymbol{k}'_\perp - \boldsymbol{k}_\perp - \boldsymbol{\ell}_\perp) - \delta(\boldsymbol{k}'_\perp - \boldsymbol{k}_\perp + \boldsymbol{\ell}_\perp)\Big]\alpha_{\mathrm{S}}(\ell_\perp^2) f(x, \ell_\perp^2)\,, \quad (11)$$

where

$$f(x, \ell^2) = \frac{\partial x G(x, \ell^2)}{\partial \ln \ell^2} \quad (12)$$

(see [14] for details). Substituting (11) into (10), we have

$$\mathcal{M}_{\lambda\lambda'} = \mathrm{i}\frac{2\pi^2 s}{\sqrt{N_{\mathrm{c}}}}\int \frac{\mathrm{d}\ell_\perp^2}{\ell_\perp^4}\alpha_{\mathrm{S}}(\ell_\perp^2) f(x, \ell_\perp^2)\Delta\psi_{\lambda\lambda'}\,, \quad (13)$$

where the definition of $\Delta\psi$ is to be understood from (10)–(13):

$$\Delta\psi = 2\psi(\boldsymbol{k}_\perp, z) - \psi(\boldsymbol{k}_\perp - \boldsymbol{\ell}_\perp, z) - \psi(\boldsymbol{k}_\perp + \boldsymbol{\ell}_\perp, z)\,. \quad (14)$$

$\psi_{\lambda\lambda'}$ has been calculated in [14] both for a transverse and a longitudinal polarized incoming photon. The wave function for a transverse polarized photon and the amplitude for producing $\bar{\mathrm{q}}$q with helicities λ and λ' read:

$$\psi^{\pm}_{\lambda\lambda'}(\mathbf{k}_\perp, z) = -\delta_{\lambda,-\lambda'} Z_f \mathrm{e}\,[(1-2z)\lambda \mp 1]\,\frac{2\epsilon_\pm \cdot k_\perp}{\bar{Q}^2 + k_\perp^2}, \quad (15)$$

$$\mathcal{M}^{\pm}_{\lambda\lambda'} = -2Z_f \mathrm{e}\left(\mathrm{i}\frac{2\pi^2 s}{\sqrt{N_{\mathrm{c}}}}\right)\delta_{\lambda,-\lambda'}\,[(1-2z)\lambda \mp 1]\,\epsilon_\pm \cdot k_\perp \times \int \frac{\mathrm{d}\ell_\perp^2}{\ell_\perp^4}\alpha_{\mathrm{S}}(\ell_\perp^2) f(x, \ell_\perp^2)\left\{\frac{1}{Q^2 + {k_\perp}^2} - \frac{1}{2{k_\perp}^2} + \frac{Q^2 - {k_\perp}^2 + \ell_\perp^2}{2{k_\perp}^2\sqrt{\left(Q^2 + {k_\perp}^2 + \ell_\perp^2\right)^2 - 4{k_\perp}^2\ell_\perp^2}}\right\}. \quad (16)$$

In (15) and (16), Z_f is the charge of the quark with flavor f in units of the electron charge $-e$, $\bar{Q}^2 \equiv z(1-z)Q^2$ and $\epsilon_\pm$ denotes the photon polarization vector presented in a circular basis,

$$\epsilon_\pm = \frac{1}{\sqrt{2}}\,(0, 0, 1, \pm\mathrm{i})\,. \quad (17)$$

To evaluate the cross section one should first sum over the quark helicities λ and λ', and average over the two transverse polarization states ($\pm$) of the photon

$$|\mathcal{M}^T|^2 = \frac{32\pi^4 s^2}{N_{\mathrm{c}}} Z_f^2 e^2\left[z^2 + (1-z)^2\right] \times \int \frac{\mathrm{d}\ell_\perp^2}{\ell_\perp^4}\alpha_{\mathrm{S}}(\ell_\perp^2) f(x, \ell_\perp^2) \times \left\{\frac{{k_\perp}^2 - \bar{Q}^2}{{k_\perp}^2 + \bar{Q}^2} + \frac{\bar{Q}^2 - {k_\perp}^2 + \ell_\perp^2}{\sqrt{\left(\bar{Q}^2 + {k_\perp}^2 + \ell_\perp^2\right)^2 - 4{k_\perp}^2\ell_\perp^2}}\right\}. \quad (18)$$

The cross section is obtained by integration over z and over $k_\perp$,

$$\sigma_{\rm T} = \frac{\alpha_{\rm em}}{4\pi^2 N_{\rm c}} \int_0^1 {\rm d}z \left[z^2 + (1-z)^2\right] \int \frac{{\rm d}k_\perp^2}{\bar{Q}^2 + k_\perp^2} \times \int \frac{{\rm d}\ell_\perp^2}{\ell_\perp^4} \alpha_{\rm S}(\ell_\perp^2) f(x, \ell_\perp^2) \times \left\{ \frac{{k_\perp}^2 - \bar{Q}^2}{{k_\perp}^2 + \bar{Q}^2} + \frac{\bar{Q}^2 - {k_\perp}^2 + \ell_\perp^2}{\sqrt{\left(\bar{Q}^2 + {k_\perp}^2 + \ell_\perp^2\right)^2 - 4{k_\perp}^2 \ell_\perp^2}} \right\}. \quad (19)$$

Following [6], in order to perform the integration over z, we introduce the variables M and $\tilde{M}$:

$$M^2 = \frac{k_\perp^2}{z(1-z)}$$
$$\tilde{M}^2 = \frac{\ell_\perp^2}{z(1-z)}, \quad (20)$$

and rewrite the integrals of $\sigma_{\rm T}$ in terms the variables M, $\tilde{\mathbf{M}}$ and $\ell_\perp$,

$$\sigma_{\rm T} = \frac{\alpha_{\rm em}}{4\pi^2 N_{\rm c}} \int \frac{{\rm d}M^2}{Q^2 + M^2} \int \frac{{\rm d}\tilde{M}^2}{\tilde{M}^2} \int \frac{{\rm d}\ell_\perp^2}{\ell_\perp^2} \frac{1 - 2\frac{\ell_\perp^2}{\tilde{M}^2}}{\sqrt{1 - 4\frac{\ell_\perp^2}{\tilde{M}^2}}} \times \alpha_{\rm S}(\ell_\perp^2) f(x, \ell_\perp^2) \times \left\{ \frac{M^2 - Q^2}{M^2 + Q^2} + \frac{Q^2 - M^2 + \tilde{M}^2}{\sqrt{\left(Q^2 + M^2 + \tilde{M}^2\right)^2 - 4M^2\tilde{M}^2}} \right\}. \quad (21)$$

Using a generalization of the Gribov approach, we take a cutoff on the integration over M^2 and insert the ratio (2) inside the integration sign,

$$\sigma_{\rm T}^{\rm hard} = \frac{\alpha_{\rm em}}{2\pi^2 N_{\rm c}} \int_{M_0^2}^\infty \frac{{\rm d}M^2\, R(M^2)}{Q^2 + M^2} \int \frac{{\rm d}\tilde{M}^2}{\tilde{M}^2} \times \int \frac{{\rm d}\ell_\perp^2}{\ell_\perp^2} \frac{1 - 2\frac{\ell_\perp^2}{\tilde{M}^2}}{\sqrt{1 - 4\frac{\ell_\perp^2}{\tilde{M}^2}}} \alpha_{\rm S}(\ell_\perp^2) f(x, \ell_\perp^2) \times \left\{ \frac{M^2 - Q^2}{M^2 + Q^2} + \frac{Q^2 - M^2 + \tilde{M}^2}{\sqrt{\left(Q^2 + M^2 + \tilde{M}^2\right)^2 - 4M^2\tilde{M}^2}} \right\}. \quad (22)$$

The last integral in (22) can be integrated by parts, using (12). In the limit $4\ell_\perp^2 \ll \tilde{M}^2$, the value of the integral is dominated by the upper limit of the integration, therefore we replace $\ell_\perp^2$ in $\alpha_{\rm S}(\ell_\perp^2)$ and $xG(x, \ell_\perp^2)$ with $\tilde{M}^2/4$, and obtain, for three colors,

$$\sigma_{\rm T}^{\rm hard} = \frac{2\pi\,\alpha_{\rm em}}{3} \int_{M_0^2}^\infty \frac{{\rm d}M^2\, R(M^2)}{Q^2 + M^2} \times \int_0^\infty \frac{{\rm d}\tilde{M}^2}{\tilde{M}^4} \alpha_{\rm S}(\frac{\tilde{M}^2}{4})\, x\, G(x, \frac{\tilde{M}^2}{4}) \times \left\{ \frac{M^2 - Q^2}{M^2 + Q^2} + \frac{Q^2 + \tilde{M}^2 - M^2}{\sqrt{(Q^2 + M^2 + \tilde{M}^2)^2 - 4M^2\,\tilde{M}^2}} \right\}. \quad (23)$$

In the case of heavy quarks, we assume that the quark is heavy enough so that any contribution to the soft cross section can be neglected. The heavy quark contribution is then written with the replacements: $4\,M^2\,\tilde{M}^2 \to 4\,(M^2 - 4m_Q^2)\,\tilde{M}^2$, and $R(Q^2) \to R^{QQ}(M^2)$. R^{QQ} is the heavy quark contribution to the ratio (2) and m_Q is the mass of the heavy quark,

$$\sigma_{{\rm T},\bar{Q}Q}^{\rm hard} = \frac{2\pi\,\alpha_{\rm em}}{3} \int_{M_0^2}^\infty \frac{{\rm d}M^2 R^{QQ}(M^2)}{Q^2 + M^2} \int_0^\infty \frac{{\rm d}\tilde{M}^2}{\tilde{M}^4} \times \alpha_{\rm S}\left(\frac{\tilde{M}^2}{4}\right) xG\left(x, \frac{\tilde{M}^2}{4}\right) \left\{ \frac{M^2 - Q^2}{M^2 + Q^2} + \frac{Q^2 + \tilde{M}^2 - M^2}{\sqrt{(Q^2 + M^2 + \tilde{M}^2)^2 - 4(M^2 - 4m_Q^2)\tilde{M}^2}} \right\}. \quad (24)$$

In the above formulas, $x = x(M^2) = (Q^2 + M^2)/W^2$ with W being the center-of-mass energy of the photon–nucleon interaction.

2.2 The contribution of a longitudinal polarized photon

2.2.1 Soft contribution to $\sigma_{\rm L}$

A priori, it is straightforward to write the formula for the soft component of $\sigma_{\rm L}$ in AQM. The result is similar to our model for $\sigma_{\rm T}$, except that M^2 in the numerator should be replaced with the photon virtuality. This factor causes the longitudinal cross section to vanish for $Q^2 \to 0$ (see (7) for the values of the parameters).

$$\sigma_{\rm L}^{\rm soft} = \frac{\alpha_{\rm em}}{3\pi} \int_0^{M_0^2} \frac{R(M^2) Q^2 {\rm d}M^2}{\left(Q^2 + M^2\right)^2} \times \left\{ A(\frac{1}{x_M})^{\alpha_{\mathbb{P}}(0)\,-\,1} + B\,(\frac{1}{x_M})^{\alpha_{\mathbb{R}}(0)\,-\,1} \right\}. \quad (25)$$

However, it turns out that the AQM overestimates the experimental data, and it has to be reduced with some phenomenological procedure, such as a numerical factor [15] or a phenomenological function which decreases with Q^2 [10]. In our formalism, the ratio between the AQM and pQCD contributions depends on the separation parameter M_0. Thus, by lowering the value of M_0, one suppresses the soft component. We have found that for the longitudinal part of the cross section, taking any value of M_0 that is below the resonance mass fits the experimental data, as opposed to the transverse cross section where we used $0.7 < M_0^2 < 0.9\,{\rm GeV}^2$.

2.2.2 Hard contribution to $\sigma_{\rm L}$

We calculate the pQCD contribution for $\sigma_{\rm L}$ from the diagrams of Fig. 3 using (10)–(14). For the case of a longitudinal polarized incoming photon, we use the expression derived in [14] for the wave function

$$\psi^{\rm L}_{\lambda\lambda'} = -2\delta_{\lambda,-\lambda'} Z_f {\rm e} Q z(1-z) \frac{1}{\bar{Q}^2 + k_\perp^2}, \qquad (26)$$

and substitute it in (13) to obtain the amplitude for a longitudinal photon to produce $\bar{\rm q}$q with helicities λ and λ'

$$\begin{aligned}
&\mathcal{M}^{\rm L}_{\lambda\lambda'} \\
&= -4\delta_{\lambda,-\lambda'} Z_f {\rm e} Q z(1-z) {\rm i} \frac{2\pi^2 s}{\sqrt{N_{\rm c}}} \\
&\times \int \frac{{\rm d}\ell_\perp^2}{\ell_\perp^4} \alpha_{\rm S}(\ell_\perp^2) f(x, \ell_\perp^2) \\
&\times \left\{ \frac{1}{\bar{Q}^2 + {k_\perp}^2} - \frac{1}{\sqrt{\left(\bar{Q}^2 + {k_\perp}^2 + \ell_\perp^2\right)^2 - 4{k_\perp}^2 \ell_\perp^2}} \right\}. \qquad (27)
\end{aligned}$$

The cross section is then obtained by squaring, summing over the final helicities and integrating over z and $k_\perp$,

$$\begin{aligned}
\sigma_{\rm L} = &\frac{16\pi\alpha_{\rm em}}{N_{\rm c}} \sum Z_f^2 Q^2 \int_0^1 {\rm d}z \left[z(1-z)\right]^2 \int \frac{{\rm d}k_\perp^2}{\bar{Q}^2 + k_\perp^2} \\
&\times \int \frac{{\rm d}\ell_\perp^2}{\ell_\perp^4} \alpha_{\rm S}(\ell_\perp^2) f(x, \ell_\perp^2) \qquad (28) \\
&\times \left\{ \frac{1}{\bar{Q}^2 + {k_\perp}^2} - \frac{1}{\sqrt{\left(\bar{Q}^2 + {k_\perp}^2 + \ell_\perp^2\right)^2 - 4{k_\perp}^2 \ell_\perp^2}} \right\}.
\end{aligned}$$

Changing the integration variables $k_\perp^2$ and $\ell_\perp^2$ to M and $\tilde{M}$, respectively, using (20), we have

$$\begin{aligned}
\sigma_{\rm L} = &\frac{16\pi\alpha_{\rm em}}{N_{\rm c}} \sum Z_f^2 Q^2 \int_0^1 {\rm d}z \int \frac{{\rm d}M^2}{Q^2 + M^2} \\
&\times \int \frac{{\rm d}\tilde{M}^2}{\tilde{M}^4} \alpha_{\rm S}(z(1-z)\tilde{M}^2) f(x, z(1-z)\tilde{M}^2) \qquad (29) \\
&\times \left\{ \frac{1}{Q^2 + M^2} - \frac{1}{\sqrt{\left(Q^2 + M^2 + \tilde{M}^2\right)^2 - 4M^2\tilde{M}^2}} \right\}.
\end{aligned}$$

We now write the formula for $\sigma_{\rm L}^{\rm hard}$ in the same way that we did in Sect. 2.1, by taking a cutoff on the integration over M^2, and insert the ratio (2) inside the integration sign,

$$\begin{aligned}
&\sigma_{\rm L}^{\rm hard} \\
&= \frac{8\pi\alpha_{\rm em}}{N_{\rm c}} Q^2 \int_{M_0^2}^\infty \frac{R(M^2){\rm d}M^2}{Q^2 + M^2} \int_0^\infty \frac{{\rm d}\tilde{M}^2}{\tilde{M}^4} \\
&\times \int_0^1 {\rm d}z f\left(x, z(1-z)\tilde{M}^2\right) \alpha_{\rm S}\left(z(1-z)\tilde{M}^2\right) \\
&\times \left\{ \frac{1}{Q^2 + M^2} - \frac{1}{\sqrt{\left(Q^2 + M^2 + \tilde{M}^2\right)^2 - 4M^2\tilde{M}^2}} \right\}. \qquad (30)
\end{aligned}$$

Recalling (12), we can integrate (30) by parts and obtain (for $N_{\rm c} = 3$),

$$\begin{aligned}
\sigma_{\rm L}^{\rm hard} = &\frac{8\pi\alpha_{\rm em}}{3} Q^2 \int_{M_0^2}^\infty \frac{R(M^2){\rm d}M^2}{Q^2 + M^2} \int_0^\infty \frac{{\rm d}\tilde{M}^2}{\tilde{M}^4} \overline{xG}\left(x, \tilde{M}^2\right) \\
&\times \left\{ \frac{1}{Q^2 + M^2} - \frac{1}{\sqrt{(Q^2 + M^2 + \tilde{M}^2)^2 - 4M^2\tilde{M}^2}} \right. \\
&\left. - \frac{\tilde{M}^2\left(Q^2 + \tilde{M}^2 - M^2\right)}{\left(\sqrt{(Q^2 + M^2 + \tilde{M}^2)^2 - 4M^2\tilde{M}^2}\right)^3} \right\}, \qquad (31)
\end{aligned}$$

where

$$\begin{aligned}
\overline{xG}\left(x, \tilde{M}^2\right) \equiv &\int_0^1 xG\left(x, z(1-z)\tilde{M}^2\right) \\
&\times \alpha_{\rm S}\left(z(1-z)\tilde{M}^2\right) {\rm d}z\,. \qquad (32)
\end{aligned}$$

For $\sigma^{\rm hard}_{{\rm L},\bar{Q}Q}$, the contribution of heavy quarks to the longitudinal component of $\sigma(\gamma^*{\rm p})$, we replace $4M^2\tilde{M}^2$ by $4(M^2 - 4m_Q^2)\tilde{M}^2$ and $R(Q^2)$ with $R^{QQ}(M^2)$, as we did for the transverse part:

$$\begin{aligned}
&\sigma^{\rm hard}_{{\rm L},\bar{Q}Q} \\
&= \frac{8\pi\alpha_{\rm em}}{3} Q^2 \int_{M_0^2}^\infty \frac{R^{QQ}(M^2){\rm d}M^2}{Q^2 + M^2} \\
&\times \int_0^\infty \frac{{\rm d}\tilde{M}^2}{\tilde{M}^4} \overline{xG}\left(x, \tilde{M}^2\right) \left\{ \frac{1}{Q^2 + M^2} \right. \\
&- \frac{1}{\sqrt{(Q^2 + M^2 + \tilde{M}^2)^2 - 4(M^2 - 4m_Q^2)\tilde{M}^2}} \\
&\left. \times \frac{\tilde{M}^2\left(Q^2 + \tilde{M}^2 - M^2\right)}{\left(\sqrt{(Q^2 + M^2 + \tilde{M}^2)^2 - 4(M^2 - 4m_Q^2)\tilde{M}^2}\right)^3} \right\}. \qquad (33)
\end{aligned}$$

3 Comparison with the experimental data

We now present the results for our calculation of $\sigma(\gamma^*{\rm p})$ from the master equation

$$\begin{aligned}
\sigma(\gamma^*{\rm p}) = &\sigma_{\rm T}^{\rm soft} + \sigma_{\rm T}^{\rm hard} + \sigma_{{\rm T},\bar{Q}Q}^{\rm hard} \\
&+ \sigma_{\rm L}^{\rm soft} + \sigma_{\rm L}^{\rm hard} + \sigma_{{\rm L},\bar{Q}Q}^{\rm hard}\,. \qquad (34)
\end{aligned}$$

As stated, our model has three parameters, namely, $M_{0,{\rm L}}, M_{0,{\rm T}}$, and μ. In [6], the relatively high value of

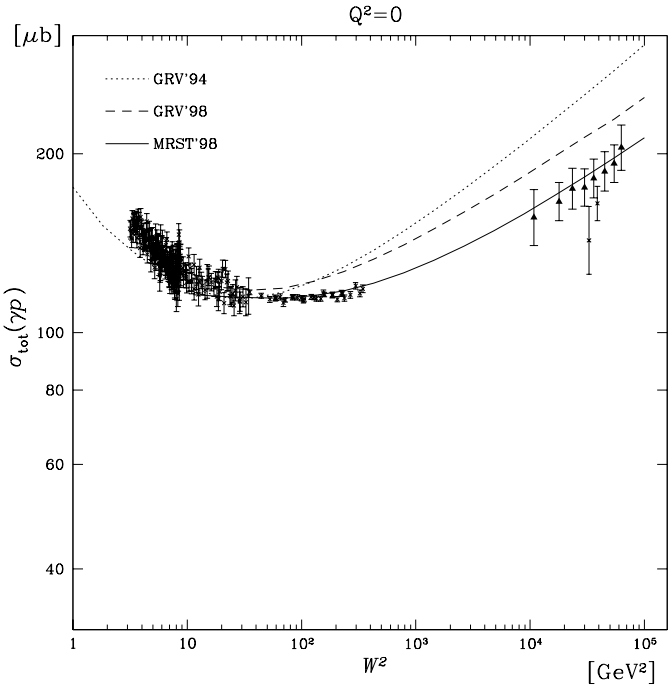

Fig. 4. Comparison of the gluon distribution parameterizaions which were used in (34) to calculate $\sigma(\gamma^*\mathrm{p})$. The full triangles correspond to data points which have been extracted in [19] from experimental data

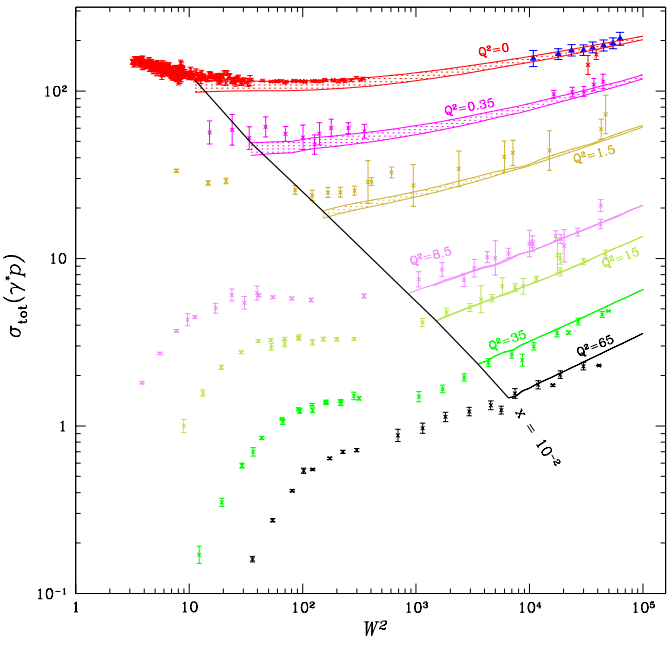

Fig. 5. $\sigma(\gamma^*\mathrm{p})$ as a function of W^2, together with the experimental data. The full triangles correspond to data points that have been extracted in [19] from experimental data

$M_0 = \sqrt{5}$ GeV was taken, in order to give an energy dependence that was in a reasonable agreement with the published experimental results. We found that if the hard longitudinal contributions are not neglected, the transverse separation parameter can be reduced to the value of $0.7 < M^2_{0,\mathrm{T}} < 0.9$ GeV^2, while the longitudinal one can be taken to be $M^2_{0,\mathrm{L}} \lesssim 0.4$ GeV^2. The results of the calculation are stable if the separation parameters are chosen within these bounds.

In the calculation of the hard components of $\sigma(\gamma^*\mathrm{p})$, we need to specify the input gluon distribution $xG(x,Q^2)$ which appears in the formulas. We have tried several options: GRV'94 [16], GRV'98 [17] and MRST'98 [18]. We compare the results of each input distribution for the calculation of $\sigma(\gamma p)$ in Fig. 4, where it is obvious that the best parameterization for our purpose is MRST '98, which yields, together with our formalism, a good description of the data.

A difficulty in our calculation comes from the integration at very low M^2, where the published parameterizations for xG are not valid. Naturally one has two possible options: The first is to impose a low cutoff on the integration below $M^2 = \mu^2$. The second option is to use the general property of the gluon structure function, which is linear in Q^2 at very small values of Q^2, and to rely on this property for the low-mass region:

$$xG(x, l^2 < \mu^2) = \frac{l^2}{\mu^2} xG(x, \mu^2)\,. \qquad (35)$$

In our calculation for the low mass integration, we used (35) for the gluon distribution. The coupling $\alpha_{\mathrm{S}}(Q^2)$ was also kept fixed for $Q^2 < \mu^2$. The value of μ^2 was taken as the minimal value allowed in the input parameterization used: $\mu^2 = 0.4, 0.8, 1.25$ GeV^2 for GRV '94, GRV '98, and MRST '98 respectively. Notice that for the MRST parameterization $\mu^2 = 1.25\,\mathrm{GeV}^2 > M_0^2$. This means that the transition from soft to hard is not sharp, and we still have (35) as a soft signature inside our hard formalism at $M_0^2 < M^2 < \mu^2$.

In Fig. 5, we show the results of our calculation for $\sigma(\gamma^*\mathrm{p})$ as a function of W^2 for fixed values of Q^2, together with the published experimental results. The calculated results are shown as a band which corresponds to the two limits on $M_{0,\mathrm{T}}$. It is clear from the figure that the width of the band decreases with increasing Q^2. As for the longitudinal separation parameter, the results are not sensitive to the choice of $M_{0,\mathrm{L}}$, and in all our calculations we simply used $M_{0,\mathrm{L}} = 2m_\pi$. The thick line marks the region of small x: to the left of it, x is not small enough to justify use of our model. One can see that for $x < 10^{-2}$, our results reproduce the experimental results both in value and in energy dependence.

In Fig. 6, we show our calculations for $\sigma(\gamma^*\mathrm{p})$ for fixed values of W^2 as a function of Q^2, scaled by factors of 1–128. The small vertical thick lines delineate the boundary $x = 10^{-2}$; to the right of the marks, our results are not reliable.

The longitudinal component of $\sigma(\gamma^*\mathrm{p})$, according to our calculation, reaches a maximum value of 25% of the total cross section at $x \approx 10^{-2}$. For small x, this result is closer to the published data [20] than the results of [10], where they obtained σ_{L} for $x \approx 10^{-2}$ to be 15% of

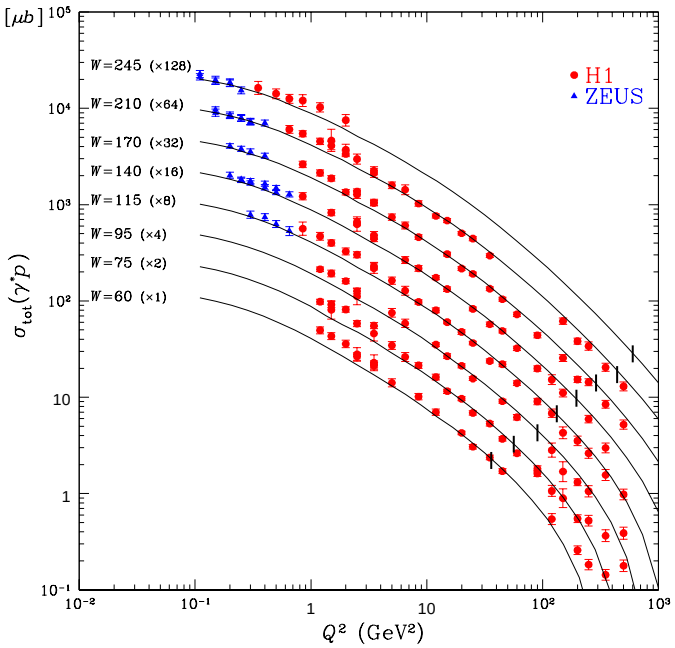

Fig. 6. $\sigma(\gamma^*\mathrm{p})$ as a function of Q^2, together with the experimental data

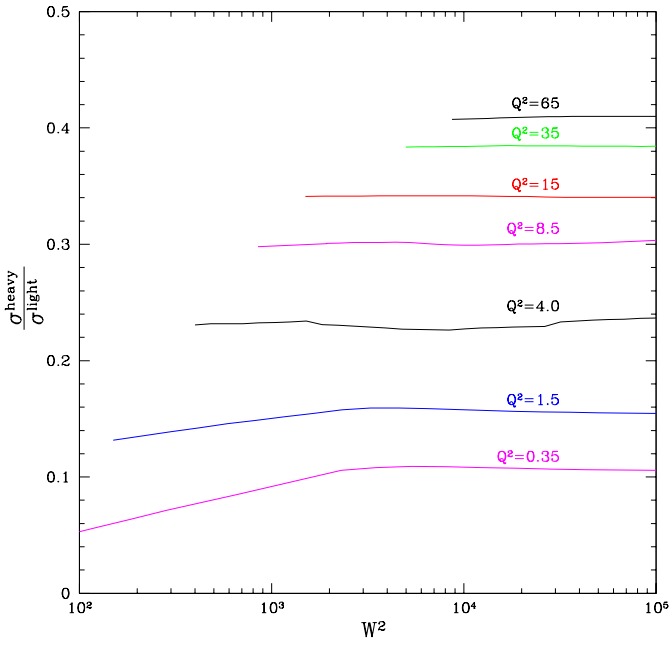

Fig. 8. The ratio of $\frac{\sigma^{\mathrm{heavy}}}{\sigma^{\mathrm{light}}}$ at fixed Q^2

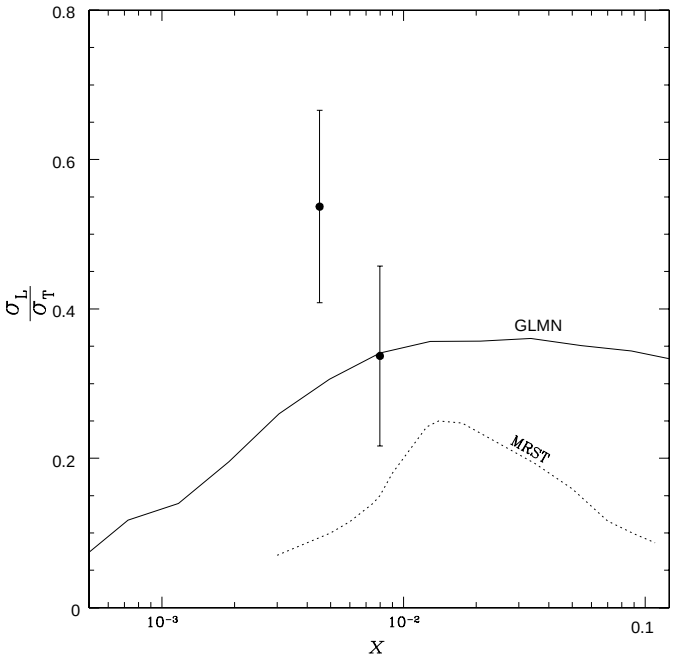

Fig. 7. The ratio of $\frac{\sigma_{\mathrm{L}}}{\sigma_{\mathrm{T}}}$ as a function of x

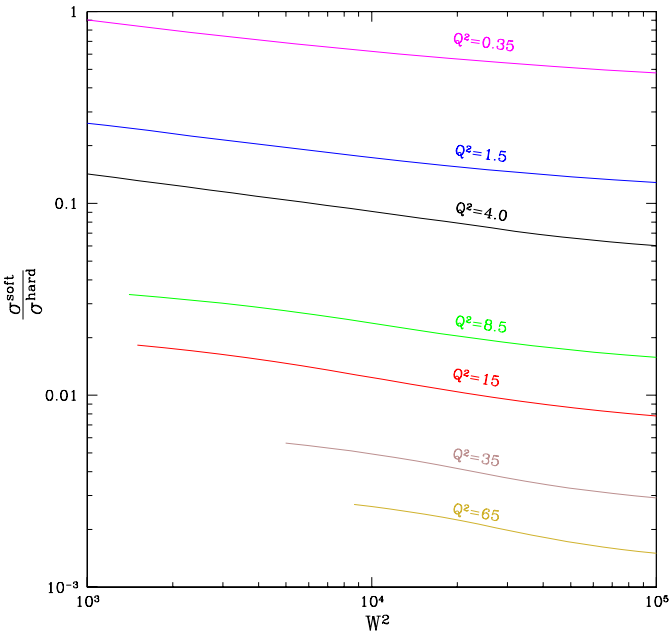

Fig. 9. The ratio of $\frac{\sigma^{\mathrm{soft}}}{\sigma^{\mathrm{hard}}}$ at fixed Q^2

the total cross section. The ratio of the longitudinal cross section to the transverse cross section, as a function of x, is shown in Fig. 7 together with the (small x) data of [20].

Figure 8 illustrates the importance of the heavy quarks contributions $\sigma^{\mathrm{hard}}_{\mathrm{T},\bar{Q}Q}$ and $\sigma^{\mathrm{hard}}_{\mathrm{L},\bar{Q}Q}$ (see (24) and (33)). The contribution has a mild W^2 dependence, but it is Q^2-dependent, and for large Q^2, the ratio $\sigma^{\mathrm{heavy}}/\sigma^{\mathrm{light}}$ gets as high as 0.3–0.4. We present also the ratio of hard to soft contributions. Since $M_{0,\mathrm{L}}$ is smaller than the lightest resonance mass, the AQM contribution to the longitudinal component is suppressed, and therefore what we call a soft contribution is actually the transverse AQM calculation.

In Fig. 9, we present the ratio $\sigma^{\mathrm{soft}}/\sigma^{\mathrm{hard}}$ at fixed values of Q^2, where a clear power law behavior as a function of W^2 can be seen. In soft processes, the hard contribution is minor but is still present even for relatively small values of Q^2. The soft signature in hard processes is also present, but is smaller. For high virtualities it decreases from a few percent at low energy, to less than 1% at high energies.

4 Conclusions

In this paper, we have shown that an approach based on Gribov's proposal provides a successful description of the experimental data on photon–proton interaction, over a wide range of photon virtualities $0 \leq Q^2 \leq 100$ GeV^2, and energies $3 \leq \sqrt{s}\,(= W) \leq 300$ GeV. The key assumption on which our approach is based is that the nonperturbative and the perturbative QCD contributions in the Gribov formula can be separated by the parameter M_0. Our successful reproduction of the experimental data (see Figs. 5 and 6) shows that this assumption appears to be valid. It further lends credence to use of the additive quark model (AQM) to describe the nonperturbative contribution. The successful use of the AQM leads to an improved result in this paper, as compared to our previous result [6], where we found it necessary to introduce a damping factor for the AQM.

The second important by-product of our calculation is the simple method we have used to distinguish between nonperturbative (soft) and perturbative (hard) contributions. We have used three separation parameters: $M_{0,\mathrm{T}}$, $M_{0,\mathrm{L}}$ and μ. The values of these parameters, $M^2_{0,\mathrm{T}} = 0.7 - -0.9$ GeV^2, $M^2_{0,\mathrm{L}} \leq 0.4$ GeV^2 and $\mu^2 \approx 1$ GeV^2, were determined by fitting to the experimental data. We believe that these values may be useful in the future for a more theoretical description of the matching between soft and hard processes in QCD.

The third result we find interesting is that the GRV parameterizations of the structure functions cannot successfully describe the experimental energy dependence of the total cross section at small values of Q^2 (see Fig. 4), while the MRST parameterizations can. This result shows the interdependence of deep inelastic scattering data, and the theoretical description of the matching of the soft and hard contributions.

In addition, we obtain the following:

1. A description of the ratio $\sigma_{\mathrm{L}}/\sigma_{\mathrm{T}}$ (see Fig. 7) that is in good agreement with the experimental data and other approaches. The fact that σ_{L} appears to have only a hard contribution should be stressed, as this could be a possible window for particular features of nonperturbative QCD.
2. A considerable contribution of the soft processes at rather large values of photon virtualities Q^2. For example at $Q^2 = 15$ GeV^2 and $\sigma^{\mathrm{soft}}/\sigma^{\mathrm{hard}} \approx 4\%$ at $W = 10$ GeV (see Fig. 9). We also find, at low Q^2, a contamination of the soft processes by the hard ones. For high-energy real photoproduction, this contamination amounts to about 5%. We believe that this fact should be taken into account when interpreting experimental data, especially as far as their energy dependence is concerned.
3. The prediction of the cross section for the heavy-quark production (see Fig. 8) which is almost W-independent, while showing a steep Q^2 decrease.

We propose a simple and successful phenomenological model for the photon–proton interaction, which provides a method for matching the soft and hard interactions at high energy, and which can be a guide for future theoretical approaches. It is worth mentioning that even in its present form, our model can be useful for determining the initial parton distributions at leading twist for the DGLAP evolution equations.

Acknowledgements. We thank A. Martin and A. Stasto for useful discussions of the results of this paper, and for providing us the kumac file for Fig. 6. This research was supported in part by the Israel Science Foundation, founded by the Israel Academy of Science and Humanities.

References

1. H1 Collaboration: C. Adloff, et al.,Nucl. Phys.**B497** (1997) 3; H1 Collaboration: S. Aid, et al.,Nucl. Phys.**B470** (1996) 3
2. ZEUS Collaboration: J. Breitweg, et al., Phys. Lett.**B407** (1997) 432
3. V.N. Gribov, Sov. Phys.JETP**30** (1970) 709
4. J.J. Sakurai and D. Schildknecht, Phys. Lett.**B40** (1972) 121; B. Gorczyca and D. Schildknecht, Phys. Lett.**B47** (1973) 71
5. Particle Data Group, Eur. Phys. J. C **3**, 1 (1998)
6. E. Gotsman, E.M. Levin, and U. Maor, Eur. Phys. J.**C5** (1998) 303
7. B. Badelek and J. Kwiecinski, Z. Phys.**C43** (1989) 251,Phys. Lett.**B295** (1992) 263,Phys. Rev.**D50** (1994) R4
8. E.M. Levin and L.L. Frankfurt, JETP Letters **3** (1965) 652; H.J. Lipkin and F. Scheck, Phys. Rev. Lett. **16** (1966) 71; J.J.J. Kokkedee, *The Quark Model* (NY, W.A. Benjamin 1969)
9. A. Donnachie and P.V. Landshoff, Nucl. Phys.**B244** (1984) 322,Nucl. Phys.**B267** (1986) 690, Phys. Lett.**B296** (1992) 227,Z. Phys.**C61** (1994) 139
10. A.D. Martin, M.G. Ryskin, and A.M. Stasto, DTP/98/20; `hep-ph/9806212`.
11. K. Golec-Biernat and M. Wüsthoff,Phys. Rev.**D59** (1999) 014017
12. H. Abramowicz, E. Levin, A. Levy, and U. Maor, Phys. Lett.**B269** (1991) 465
13. H. Abramowicz and A. Levy, DESY 97-251, `hep-ph/9712415`
14. E.M. Levin, A.D. Martin, M.G. Ryskin, and T. Teubner, Z. Phys.**C74** (1997) 671
15. D. Schildknecht, H. Spiesberger, BI-TP 97/25, `hep-ph/9707447`
16. M. Gluck, E. Reya, and A. Vogt, Z. Phys.**C67** (1995) 433
17. M. Gluck, E. Reya, and A. Vogt, `hep-ph/9806404`
18. A.D. Martin, R.G. Roberts, W.J. Stirling, and R.S. Thorne: *"Parton distributions: a new global analysis"*, DTP/98/10; `hep-ph/9803445`
19. ZEUS Collaboration: J. Breitweg, et al., DESY 98-121, `hep-ex/9809005`
20. NMC Collaboration, Nucl. Phys.**B483** (1997) 3